Analysis of Worst-Case Phase Quantization Sidelobes in Focused Beamforming

Sverre Holm, *Member, IEEE*, and Kjell Kristoffersen

Abstract— **The effect of phase quantization errors on the sidelobe level in a phased-array beamformer is considered. First the theory of random and periodic phase errors is reviewed. Periodic phase errors occur for an unfocused array with uniform element distance and give rise to discrete sidelobes. The main result of the paper is an analysis of the periodic phase error in the case that the beamformer is focused. An estimate for the worst-case discrete sidelobe level as a function of focal depth is derived. The theory is illustrated and verified by simulations.**

I. Introduction

In a beamformer, quantization of the time or phase delays gives rise to two effects that will degrade quality: random sidelobes and discrete sidelobes. The analysis of phase quantization errors and the resulting sidelobes is a topic that has been of concern to researchers involved with array and beamformer designs both in radar systems [1], sonar systems [6], and ultrasound systems for medical [3] and nondestructive testing applications [5]. Typical for radar and sonar applications is the absence of focusing. Therefore, in these application areas, the analysis of quantization errors has mostly been restricted to random errors and periodic errors. Random phase errors are assumed to be uncorrelated from element to element and give rise to a sidelobe structure that is also random as a function of angle and that can be characterized by a mean sidelobe level. Periodic errors occur in unfocused uniform arrays (i.e., with uniform distance between individual elements) when steered to certain directions and give rise to strong discrete sidelobes.

In ultrasound imaging, common types of linear and phased arrays have the property of uniform distance between elements. The discrete sidelobes are therefore of importance in determining the worst-case sidelobe levels. However, in order to give reliable estimates, the effect of focusing must be included. In focused imaging systems, the focusing tends to break up and randomize the periodic phase error. Therefore, focusing to a close distance will in the limit tend to give a completely uncorrelated phase error, while focusing to a large distance gives an almost periodic phase error in the worst case. This has previously been considered by Peterson and Kino [5] who presented an estimate of the sidelobe level in a focused system. Their estimate of the level is of approximately the same functional form as the one presented here, but predicts a lower level. The reason is that they only considered an unsteered system. We show here that in order to find the worst-case sidelobe levels the system has to be steered to one of the directions that give a periodic phase error as given by Gray [6].

In this paper we review the theory for random and periodic phase quantization errors. For a focused imaging system we derive a worst-case estimate of the level and location of the discrete sidelobes. This result is used to define depth regions where either random or discrete sidelobes are dominant, and to give criteria for the relationship between the number of elements in the array and the coarseness of phase quantization.

Manuscript received March 21, 1991; revised February 20, 1992; accepted April 2, 1992. This work was supported in part by Royal Norwegian Council for Scientific Research (NTNF).

S. Holm is with Vingmed Sound AS, Research Department, Vollsveien 13C, N-1324 Lysaker, Norway, and Division of Telecommunications, Norwegian Institute of Technology, N-7034 Trondheim, Norway

K. Kristoffersen is with Vingmed Sound AS, Research Department, Vollsveien 13C, N–1324 Lysaker, Norway.

IEEE Log Number 9201919.

II. Model

The effect of time or phase errors can be found by considering the time delay, low-pass beamformer:

$$b(t,\theta,r) = \sum_{n=0}^{N-1} w_n x_n(t - d_n) \tag{1}$$

where $b(t,\theta,r)$ is the beamformer output, $x_n(t)$ is the input from element number n in an array with N elements, and w_n is the weighting or apodization. The time-delay for each element, d_n, is determined by the direction, θ, that the array is steered to and in a focused system also the depth, r. When the beamformer is steered to a direction, θ off broadside in the far-field, the time delays are given by

$$d_{n,\text{steer}} = ((n - N/2)l \sin\theta)/c \tag{2}$$

where l is the interelement distance and c the velocity of sound. If the beamformer is focused at the point (r,θ), an additional focusing time delayed is added, as shown in (3), at the bottom of the following page, where the approximation is the Fresnel approximation.

In the rest of the paper a narrowband signal will be assumed. We will use complex notation in order to model the effect of errors in the down-mixed, baseband output from the beamformer. First, let the signal be a continuous sinewave of frequency $w_0 = 2\pi f_0$, received from a point source at (θ^s, r^s) with source delay d_n^s given by (2) and (3):

$$x_n(t|\theta^s, r^s) = \exp(jw_o(t + d_n^s)). \tag{4}$$

The beamformer delays found from (2) and (3) will be quantized to $\hat{d}_n = k/f_s$ where k is integer and f_s is the sampling frequency. Often in digital beamforming, interpolation is used in order to obtain an more efficient implementation [4]. If the

interpolator is of a reasonable quality, f_s is the sampling rate after interpolation. The level of the sidelobes (whether random or discrete) is given by the number of quantization steps per period of the beamformed signal, m. The oversampling ratio is $m = f_s/f_0$ i.e., the ratio of the sampling frequency and the signal frequency.

After quantization of the delay, there will be a phase error per element, e_n, in the range $[-\pi/m, \pi/m]$. The output of the beamformer can then be expressed as

$$b(t,\theta,r|\theta^s,r^s) = \exp(jw_0t)\sum_{n=0}^{N-1} w_n \cdot \exp(je_n)\cdot\exp(jw_0(d_n^s - d_n)). \quad (5)$$

Thus the desired response is seen through a phase grating. The beam pattern is obtained as the time average and when the phase errors are small, the error term may be expanded as a power series, and an approximation may be obtained by retaining the first two terms:

$$\begin{aligned} b(\theta,r|\theta^s,r^s) &= \sum_{n=0}^{N-1} w_n\cdot\cos e_n\cdot\exp(jw_0(d_n^s-d_n)) \\ &\quad + j\sum_{n=0}^{N-1} w_n\cdot\sin e_n\cdot\exp(jw_0(d_n^s-d_n)) \\ &\approx \sum_{n=0}^{N-1} w_n\cdot\exp(jw_0(d_n^s-d_n)) \\ &\quad + j\sum_{n=0}^{N-1} w_n\cdot e_n\cdot\exp(jw_0(d_n^s-d_n)). \end{aligned} \quad (6)$$

Thus, in the far-field where $(d_n^s - d_n)$ varies linearly with n as given by (2), the beam pattern consists of the desired response and an additive term that is given by the Fourier transform of the time delay error over the array. For a focused system, the Fourier transform generalizes to a focused delay sum with d_n and d_n^s given by the sum of (2) and (3), but the analysis of the effect of phase errors is essentially the same. The properties of the phase error in the two cases are however quite different as will be shown here.

The properties of the weighting function are important in the subsequent analysis and therefore some characteristics will be defined. The normalized coherent power gain (CPG) is

$$\mathrm{CPG} = \left[\frac{1}{N}\sum_{n=0}^{N-1} w_n\right]^2. \quad (7)$$

The normalized incoherent power gain (IPG) is

$$\mathrm{IPG} = \frac{1}{N}\sum_{n=0}^{N-1} w_n^2. \quad (8)$$

The ratio of the two is in spectral analysis called the normalized equivalent noise bandwidth (ENBW) [2]. In the context of spatial processing a more suitable term is equivalent noise beamwidth with the same abbreviation:

$$\mathrm{ENBW} = \frac{\mathrm{IPG}}{\mathrm{CPG}}. \quad (9)$$

The normalization implies that a rectangular weighting will give unity for all three values. The incoherent power gain lies in the range 0.25 to 0.4 for commonly used weighting functions. The equivalent noise beamwidth ranges from 1.2 to about 2.

III. Random Quantization Lobes

If the phase quantization error has a uniform distribution over the quantization range $[-\pi/m, \pi/m]$, the variance of the phase error can be found as $(2(\pi/m))^2/12 = \pi^2/(3m^2)$ [1]. The ratio of the desired response and the undesired response can be found from the first and last terms of (6). The desired signal will be coherently added in the beamformer. The error component is assumed to be uncorrelated and will therefore be incoherently added. Although the phase quantization error in a sense is deterministic since it can be predicted from the quantization process, the case when the errors on individual channels are uncorrelated implies that one can consider the error to be a realization of a white, random process. That kind of phase quantization error will therefore be referred to as random. The resulting average voltage noise to signal ratio or sidelobe level is

$$\mathrm{SL_{avg}} = \frac{\left[\sum_{n=1}^{N} w^2(n)\right]^{\frac{1}{2}}}{\sum_{n=1}^{N} w(n)}\frac{\pi}{m3^{\frac{1}{2}}} = \frac{\pi}{m}\left(\frac{\mathrm{ENBW}}{3N}\right)^{\frac{1}{2}}. \quad (10)$$

This expression has been known for a long time in the radar literature [1]. Similar effects are caused by random variations in individual channel gains and by quantization of the weighting function. In these cases it is also appropriate to assume that the amplitude errors from channel to channel are independent. In most cases it is however less expensive in terms of implementation to avoid these effects than to avoid the effects of phase quantization. The random error squared will be distributed according to a χ^2 distribution with 2 degrees of freedom (=exponential distribution). The peaks of the squared error will therefore be a factor of 4.6 above the mean (1% percentile). The peak one-way sidelobe level (voltage) is therefore:

$$\mathrm{SL_{peak}} \approx \frac{\pi}{m}\left(\frac{4.6\cdot\mathrm{ENBW}}{3N}\right)^{\frac{1}{2}}. \quad (11)$$

$$d_{n,\mathrm{focus}} = \left((r - x\sin\theta) - \left[(r-x\sin\theta)^2 + ((n-N/2)l\cos\theta)^2\right]^{\frac{1}{2}}\right) \Big/ \; c \approx -\frac{((n-N/2)l\cos\theta)^2}{2rc} \quad (3)$$

IV. Discrete Quantization Lobes in an Unfocused System

The second effect of delay quantization is discrete quantization lobes that resemble grating lobes. This occurs whenever the quantization error over the array becomes periodic. The effect is described in [1] and [6]. There are three conditions that enhance this effect:

- a regular array geometry, i.e., a uniform, noncurved linear or phased array,
- continuous wave transmission, and
- far-field operation.

The third condition is never satisfied in ultrasound imaging, and will help decrease the quantization sidelobes in a medical ultrasound system in contrast to e.g., most sonar and radar systems.

For an unfocused, uniform array, excited with CW, with element distance l, and a time delay quantization to accuracy $\tau = 1/f_s = 1/(mf_0)$, Gray [6] has given the condition for a periodic time delay quantization error over the array:

$$\left(p\tau = \frac{ql\sin\theta_{p,q}}{c}\right) \Rightarrow \sin\theta_{p,q} = \frac{p}{q}\frac{\lambda}{ml}. \tag{12}$$

In comparing with (2) it is seen that this corresponds to the case when steering of a subarray of q elements gives a time delay that is an integral number, p, of delay steps. The subarray is repeated periodically over the array when steered to direction $\theta_{p,q}$. The periodic quantization error gives rise to discrete sidelobes whose direction are given by the grating lobe direction in an array with element distance ql:

$$\sin\theta_k = k\frac{\lambda}{ql} + \sin\theta_{p,q} \quad k \in \{\ldots -2, -1, 1, 2\ldots\}. \tag{13}$$

There is a very large number of combinations of p and q that will give valid angles, and therefore it is impossible to avoid discrete quantization lobes merely by avoiding to steer the array in certain directions. A closer analysis of the quantization lobes and their level is therefore necessary.

The worst-case quantization lobe is for $q = 2$, where there will be $N/2$ periods of the quantization error as shown in Fig. 1. The worst case is that every element will have a phase quantization error of $\pm\pi/(2m)$, i.e., plus or minus half the quantization step. The angles that give worst-case quantization lobe are $\theta_{1,2}, \theta_{3,2}, \theta_{5,2}$, etc.

The ratio of sidelobe to unquantized mainlobe level is the sum of the quantization error over the N/q subarrays relative to the coherent sum of the mainlobe, which for $q = 2$ is

$$\mathrm{SL}_{q=2} = \frac{(N/2)\left(\sin\frac{\pi}{2m} + \sin\frac{\pi}{2m}\right)}{N} \approx \frac{\pi}{2m}. \tag{14}$$

This equation is a special case of the more general, but still approximate equation given by Gray [6].

When (14) is compared to (11), the result is that discrete sidelobes will dominate over the peak of the random sidelobes for arrays of size:

$$N > \frac{4}{3}\cdot 4.6 \cdot \mathrm{ENBW}. \tag{15}$$

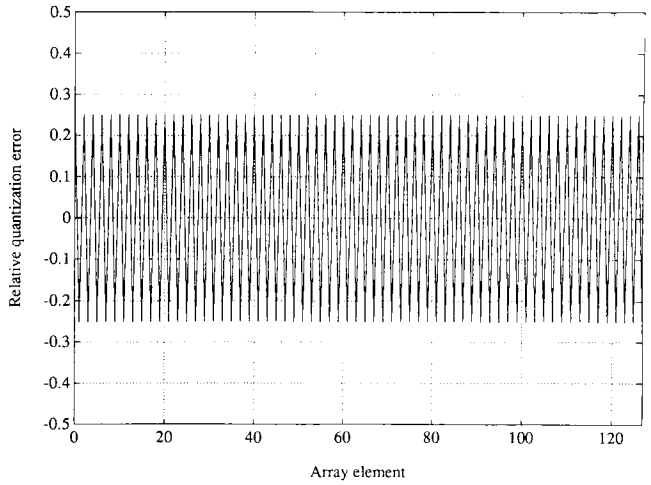

Fig. 1. Periodic time-delay quantization error normalized by the quantization step size for a uniform, unfocused array.

For practical weighting functions, all uniform arrays with more than 8 elements will be limited by the discrete quanitzation lobes in the far-field rather than the random sidelobes.

V. Sidelobes in a Focused System

In the previous two sections, the effects of random and periodic phase or time delay errors have been analyzed. In this section we discuss how focusing affects the phase errors.

When the beamformer is unfocused, the time delay increased linearly with n and in this case the phase error may become periodic. This gives rise to discrete components as expected from the Fourier transform of the phase errors according to (6).

When focusing is applied, a quadratic focusing time delay is added to the steering delay. When the focusing is at a close range, the curvature of the focus function is so large that a periodic phase error, e_n, will be completely randomized. The phase error may then be considered to be uncorrelated and the level of the sidelobes and probability distribution of the beam output can be found.

A focused system that is not steered ($\theta = 0$) will give a phase or time delay error of the type shown by the dashed line in Fig. 2. This kind of error causes sidelobes near the desired mainlobe and sometimes the only effect of them is a broadening of the mainlobe. This case was considered by Peterson and Kino [5]. However, this is not the worst case, and will not be as important as other causes of sidelobes in a focused system. This case will therefore not be discussed here.

The worst case is a combination of steering to one of the directions that gives a periodic phase error in the far-field and focusing. Furthermore, the worst case periodic phase error is when the far-field phase error alternates over the smallest possible interval, because then the periodicity is the least disturbed by the focusing. This is easily seen to be for the $\theta_{p,2}$ directions (13), where the quantization error generally will vary over $e_0 \pm \pi/(2m)$, where e_0 is a constant quantization error determined by the "phasing" between the phase to be quantized and the quantization ($e_0 = 0$ in Fig. 1). In this case, the amplitude of the far-field phase error will also

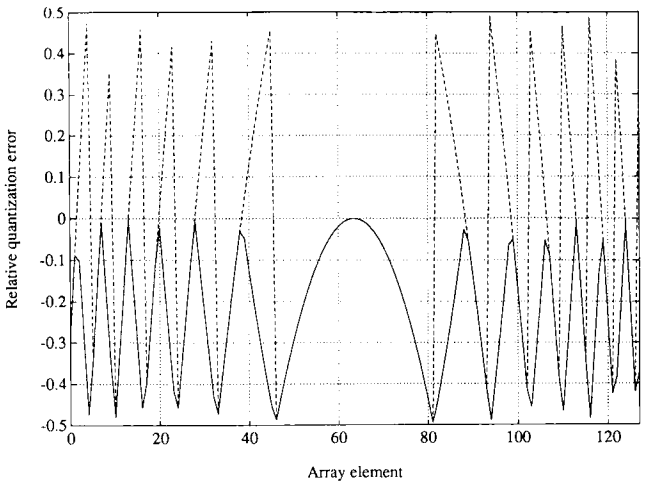

Fig. 2. Focus part of time delay quantization error normalized by the quantization step size, caused by steering and focusing (solid line) and quantization error caused by focusing alone (dashed line).

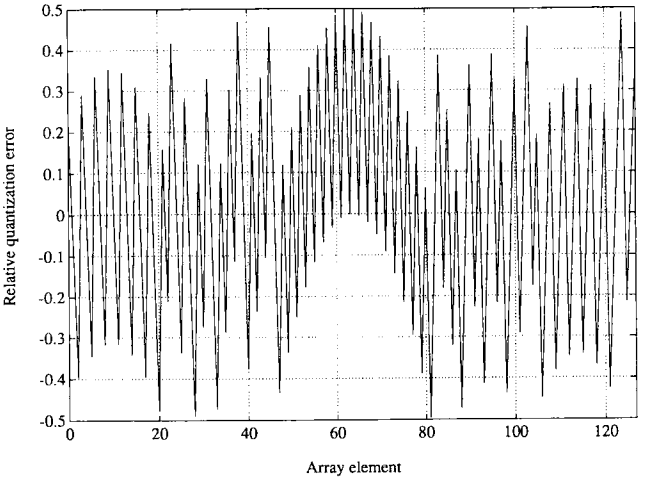

Fig. 3. Time delay quantization error normalized by the quantization step size, caused by steering and focusing.

determine the shape of the phase error due to the focusing term. Whenever the negative focusing term plus the far-field phase error, $e_{n,\text{steer}}$, is below $-\pi/m$ there will be a transition in the combined phase error. In this case one may model the net phase error (Fig. 3) as:

$$e_n = (e_{n,\text{steer}} + e_{n,\text{focus}}) \cdot \text{sign}_{\text{focus}}. \tag{16}$$

The focus term, $e_{n,\text{focus}}$ is also shown in Fig. 2 (solid line). It is equal to the phase error in a focused, unsteered system in the central part, and differs outside the central part. Its contribution to the total phase quantization error is seen in the beam pattern as a slight disturbance of the mainlobe, but this effect can be neglected in a worst-case analysis of sidelobe levels. The function $\text{sign}_{\text{focus}}$ is derived from $e_{n,\text{focus}}$ by assigning +1 to the central section of extent N_{central}, —1 to the section next to it and so on. The product of $\text{sign}_{\text{focus}}$ and a weighting function is shown in Fig. 4 (solid line). The zero crossings of this function are simple to find from the properties of a parabola, and it turns out that the distance from the center to the second transition is $\sqrt{2} \cdot N_{\text{central}}/2$, the distance to the third transition is $\sqrt{3} \cdot N_{\text{central}}/2$, and so on.

The multiplication of the previous equation translates to a convolution in the spatial domain. For a worst-case analysis, the main term in the Fourier transform of the $\text{sign}_{\text{focus}}$ term must therefore be found. The period of this term is twice the extent of the central section, $2N_{\text{central}}$. The change in the grating lobe direction due to this term is equivalent to that of a grating lobe from an array of extent $2N_{\text{central}}$, i.e., $\sin\theta_k$ of (13) will be changed by

$$\pm\lambda/(2N_{\text{central}}l) \tag{17}$$

This is the major contribution to the broadening, but not the only one. The effect of this term is that the single quantization lobe in the far-field may be split into two, depending on whether the two peaks will be resolved or not.

The worst-case focusing level reduction will be given by the Fourier transform of $\text{sign}_{\text{focus}}$ at frequency $1/2N_{\text{central}}$. Due to symmetry the Fourier transform will be real, and the

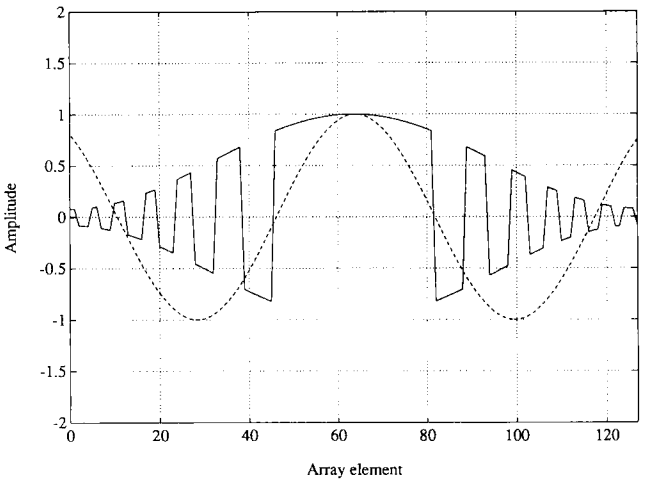

Fig. 4. Hamming weighted sign function and cosine of same fundamental period.

level reduction can be found from the correlation between the $\text{sign}_{\text{focus}}$ function and the cosine also shown in Fig. 4. It is hard to come up with a general expression for this correlation since it depends on how many periods of quantization error there are over the array and the weighting function used. An approximation may be found by considering only the central part, i.e., only half a period of the cosine. The assumption is that in the remaining sections the sign varies so rapidly compared to the cosine, that on average the net contribution is zero. This approximation is quite accurate, especially when there is a weighting function over the array that tapers down the ends as shown in Fig. 4. The approximate correlation is

$$\frac{\sum_{N_{\text{central}}} w_n \cdot \text{sign}_{\text{focus}}(n) \cdot \cos\left(2\pi \frac{n}{2N_{\text{central}}}\right)}{\sum_{N} \left(w_n \cdot \text{sign}_{\text{focus}}(n)\right)^2} = \frac{\sum_{N_{\text{central}}} w_n \cdot \cos\left(2\pi \frac{n}{2N_{\text{central}}}\right)}{\sum_{N} w_n^2}. \tag{18}$$

The approximate reduction in level relative to the estimate (14) when N_{central} is small compared to N is:

$$\frac{\sum_{N_{\text{central}}} \cos\left(2\pi \frac{n}{2N_{\text{central}}}\right)}{N \cdot \text{IPG}} \approx \frac{N_{\text{central}}}{N} \frac{\frac{1}{\pi}\int_{\frac{-\pi}{2}}^{\frac{\pi}{2}} \cos x \, dx}{\text{IPG}} = \frac{2}{\pi} \cdot \frac{N_{\text{central}}}{N} \cdot \frac{1}{\text{IPG}} \tag{19}$$

In addition, the peak splitting may give a level reduction of up to 3 dB. In a worst-case analysis, this effect will not be included. All terms combined this gives a discrete sidelobe level of

$$SL_{\text{focus}} \approx \frac{\pi}{2m} \frac{2}{\pi} \frac{N_{\text{central}}}{N} \frac{1}{\text{IPG}} = \frac{N_{\text{central}}}{Nm} \frac{1}{\text{IPG}}. \tag{20}$$

In order to find the level of the discrete quantization sidelobe, N_{central} must now be found. It is easily shown that it has its maximum value for $e_0 = \pi/m$ (which is the case illustrated in Fig. 3), and in that case the central part can be found by equating the approximate equation (3) with one half of the quantization step:

$$\left(\frac{((n - N/2)l\cos\theta)^2}{2rc} = \frac{\pi}{m}\frac{1}{2\pi f_0}\right) \Rightarrow n - N/2 = \pm\frac{N}{L\cos\theta}\left(\frac{r\lambda}{m}\right)^{\frac{1}{2}} \tag{21}$$

where $L = Nl$ is the array's aperture.

The extent of the central part of the aperture is equal to twice this value:

$$N_{\text{central}} = \frac{2N}{L\cos\theta}\left(\frac{r\lambda}{m}\right)^{\frac{1}{2}}. \tag{22}$$

Inserted in (20), this gives

$$SL_{\text{focus}} \approx \frac{2}{mL\cos\theta}\frac{1}{\text{IPG}}\left(\frac{r\lambda}{m}\right)^{\frac{1}{2}}. \tag{23}$$

This equation represents the worst-case discrete sidelobe level with focusing and is approximately reached in the case of the array being steered in the directions given by (13). It should be noted that the discrete sidelobe level is quite sensitive to the weighting function used. For instance the Hamming weighting gives a discrete sidelobe level that is 8 dB higher than the level without weighting. A Kaiser–Bessel weighting with parameter α= 3.5 (highest sidelobe level −82 dB [2]) gives a sidelobe level that is as high as 11.6 dB over that of a rectangular weighting.

It is remarkable that this equation resembles (23) in [5], although they are derived in entirely different ways. Our level estimate is much closer to the worst-case limit and more general since it includes the angle and the weighting function. Asymptotically, i.e., large m, $\theta = 0$, and rectangular weighting, our expression is a factor of 2 higher.

VI. Discussion

It is obvious that the focusing reduces the level of the discrete sidelobes, but at what depth do the discrete sidelobes become smaller than the peaks produced by random sidelobes? The answer can be found be equating (11) and (23). The result is a maximum range:

$$r_{\text{random}} = \frac{4.6 \cdot \pi^2 \cdot ENBW \cdot IPG^2}{12}\frac{(L\cos\theta)^2}{\lambda}\frac{m}{N} = a_w \cdot \frac{(L\cos\theta)^2}{\lambda}\frac{m}{N}. \tag{24}$$

For all ranges beyond this limit, the discrete sidelobes will be larger than the peak random sidelobes. The constant a_w ranges from 0.49 for Kaiser–Bessel (α = 3.5) weighting, 0.82 for Hamming weighting, and 3.8 for no weighting.

The next question is whether the above limit is inside or outside the near-field limit (transition distance) defined by

$$r_t = \frac{(L\cos\theta)^2}{4\lambda}. \tag{25}$$

If the discrete sidelobes are larger than the random sidelobes only for ranges beyond the near-field, then they will not be very important in a focused system. The answer is that the discrete sidelobes, with focusing, are important for systems where

$$N = L/l > N_1 = 4 \cdot a_w \cdot m. \tag{26}$$

This implies that only systems with a large number of elements and that operate at a high frequency (low m) will be limited by the discrete sidelobes.

The last comment concerns a uniform array designed for operation in the far-field (e.g., a sonar system). It will have a performance limited by discrete sidelobes. The level of the sidelobes may be reduced by applying focusing at for instance the transition range (the transition between the near- and the far-field). At that range $N_{\text{central}} = N/\left(m^{\frac{1}{2}}\right)$ and the discrete quantization sidelobe level is reduced by a factor of $2/\left(\pi \cdot \text{IPG} \cdot m^{\frac{1}{2}}\right)$, while the mainlobe is hardly affected.

VII. Examples

Consider the nondestructive testing system described in [5] that operates at f = 1.54 MHz, with delays quantized at $m = 5, N = 32$ elements, and aperture 40 mm. According to (24) the discrete sidelobes are of importance from a depth of 25 cm out to the transition distance at 40 cm (assuming $a_w = 1$). In [5], the system's performance was illustrated at a depth of 40 mm, which is in the region where the random sidelobes dominate.

The next example is the medical imaging digital beamformer of [3]. The time delays are quantized to 8 MHz and at a frequency of 2.5 MHz this gives an oversampling ratio of m = 3.2. The element distance is 90% of the wavelength and the aperture is 19mm. In the broadside direction this gives a limit of 5.9 cm (24). Thus at these depths and out to the transition distance at 14.7 cm, the system performance

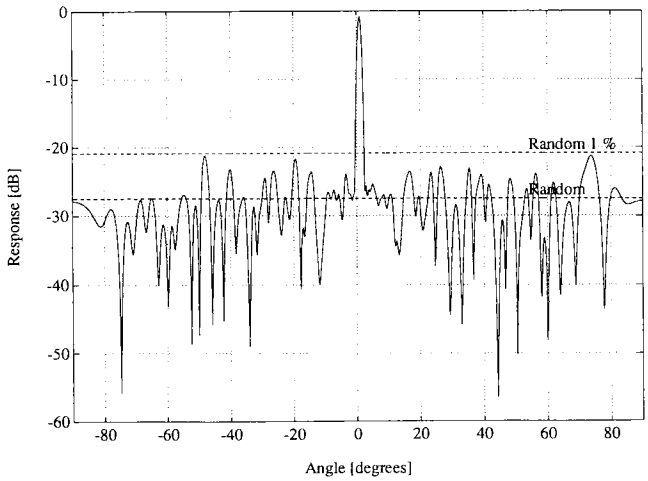

Fig. 5. Beam pattern at 5 MHz, quantization to 20 MHz, $N = 128$ elements, steered angle 1°, focal depth 20 mm.

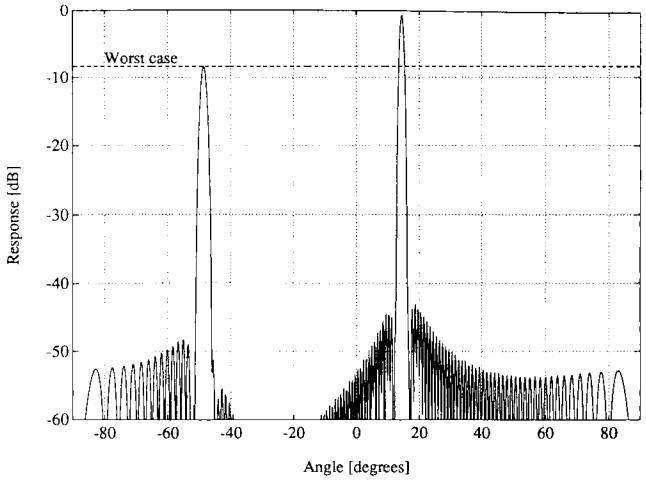

Fig. 6. Far-field beam pattern at 5 MHz, quantization to 20 Hz, $N = 128$ elements, steered angle 14.48°.

is limited by the discrete sidelobes as the paper also implicitly concludes.

A more recent medical imaging system with delays quantized to 12.5 ns accuracy is described in [7]. This is representative of the quantization level used in better ultrasound instruments. The system had only 32 elements, and the discrete sidelobes will start to limit performance for $m < 8$, i.e., signal frequencies above 10 MHz. However, if the number of elements is increased to $N = 128$, which is common in phased-array systems, the limit is $m = 32$. The discrete quantization sidelobes will therefore be present in CW mode for all frequencies above 2.5 MHz, i.e., for all commonly used medical ultrasound frequencies.

In order to illustrate the concepts of this paper a 5-MHz array system with 128 omnidirectional elements spaced half a wavelength apart has been simulated. The array output has been processed by a beamformer with a sampling rate of 20 MHz, i.e., $m = 4$, which is a rather coarse quantization. Hamming weighting is used with ENBW=1.36 and IPG=0.40. For this system, the transition distance is 31 cm, and (24) gives as a result that the worst-case sidelobe level will be determined by the discrete sidelobes for ranges beyond 3.2 cm.

Fig. 5 shows the beam pattern when the point source is moved from $\theta_s = -90°$ to $\theta_s = 90°$ and the beamformer is steered to 1° off broadside. This angle is a value that does not give any discrete quantization lobes according to (12). The mean and peak values of the expected random sidelobes are indicated and since the beamformer is focused to the as close a range as $r = r_s = 2$ cm, the resulting sidelobe level is bounded by the peak random level at −20.9 dB. Note that in this and the following examples, the loss in the mainlobe level of almost one dB is due to the relatively coarse phase quantization and the resulting inaccuracy of the approximation in (6).

Fig. 6 shows the far-field case when the beamformer is steered to $\theta_{1,2} = 14.48°$, and it is seen that the —8.3 dB level (14) of the discrete sidelobe at $\theta_{-1} = -48.6°$ (13) is an accurate estimate. The phase quantization error in this case is shown in Fig. 1.

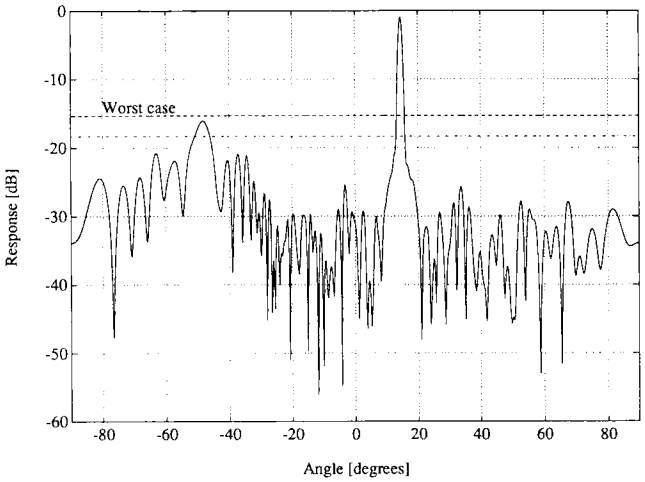

Fig. 7. Beam pattern at 5 MHz, quantization to 20 MHz, $N = 128$ elements, steered angle 14.48°, focal depth 90 mm.

In Fig. 7, the beamformer is still steered to the worst-case direction as in the previous figure, but the range has been set to 9 cm. This example corresponds to the cases illustrated in Figs. 2–4. Both the predicted discrete sidelobe level from (23) at −15.3 dB and the level 3 dB below that (corresponding to a full split of the peak) are shown. In this case also, the level of the discrete sidelobe corresponds well with the predicted value.

VIII. Conclusion

The effect of focusing on the level of the discrete time delay quantization lobes in a phased-array beamformer operating on a uniform array has been analyzed. The result is an estimate of the worst-case discrete sidelobe level in such a system. This completes the theory of discrete time delay beamforming of uniform arrays, as worst-case estimates of the quantization level both in the far-field and in the near-field are now available. The importance of this result has been discussed and

criteria on depth for when discrete sidelobes dominate over random sidelobes have been derived. A general conclusion is that the discrete sidelobes dominate over the random sidelobes for array systems where there is a large number of elements and where the time delay quantization is coarse.

ACKNOWLEDGMENT

We would like to express gratitude to Dr. Kjell Arne Ingebrigtsen of Vingmed Sound for providing the kind of environment where this research could be performed, and to Trond Kleveland of Vingmed Sound for assistance with the simulations.

REFERENCES

[1] T. C. Cheston, "Array antennas," in *Radar Handbook*, M.E. Skoknik, Ed. New York, McGraw-Hill, 1970, ch. 11.
[2] F. J. Harris, "On the use of windows for harmonic analysis with the discrete Fourier transform," *Proc. IEEE*, vol. 66, pp. 51–83, Jan. 1978.
[3] P. A. Magnin, O. T. von Ramm, and F.L. Thurstone, "Delay quantization error in phased array images," *IEEE Trans. Sonics Ultrason.*, vol. SU-28, Sept. 1981.
[4] R. A. Mucci, "A comparison of efficient beamforming algorithms," *IEEE Trans. Acoust., Speech, Signal Processing*, vol. ASSP-32, June 1984.
[5] D. K. Peterson and G. S. Kino, "Real-time digital image reconstruction: A description of imaging hardware and an analysis of quantization errors," *IEEE Trans. Sonics Ultrason.*, vol. SU-31, July 1985.
[6] D. A. Gray, "Effect of time-delay errors on the beam pattern of a linear array," *IEEE J. Ocean. Eng.*, vol. OE-10, July 1985.
[7] R. M. Lütolf, A. Vieli, and S. Basler, "Ultrasonic phased-array scanner with digital echo synthesis for Doppler echocardiography," *IEEE Trans. Ultrason., Ferroelec., Freq. Contr.*, vol. 36, Sept. 1989.

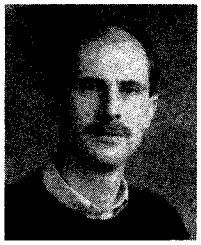

Sverre Holm (M'83) was born in Oslo, Norway, in 1954. He received the M.S. and Ph.D. degrees in electrical engineering from the Norwegian Institute of Technology, Trondheim, Norway in 1978 and 1982.

From 1978 to 1984 he did research in speech coding and spectral estimation at the Electronics Research Laboratory at the Norwegian Institute of Technology, from 1984 to 1986 he taught electrical engineering at Yarmouk University, Irbid, Jordan, and from 1986 to 1990 he was employed by Informasjonskontroll AS, Asker, Norway, doing development work in synthetic aperture radar processing and work for the European Space Agency on spectral estimation. From 1990 he has been involved in medical ultrasound research and development at Vingmed Sound AS. Since 1989 he has also been an Adjunct Professor at the Norwegian Institute of Technology. His research interests are digital signal processing, spectral estimation, and ultrasound and radar imaging.

Dr. Holm is a member of the European Association for Signal Processing (EURASIP) and the Norwegian Society for Signal Processing (NORSIG) and served as vice-president of NORSIG in 1987–1989.

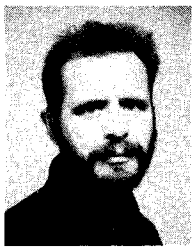

Kjell Kristoffersen was born in Karmøy, Norway, in 1952. He received the M.S. and Dr. Techn. degrees from the Norwegian Institute of Technology, Trondheim, Norway in 1978 and 1986, respectively.

From 1978 to 1984 he worked with research and development in several areas of process identification and Doppler ultrasound at the Division of Automatic Control, SINTEF, Trondheim, Norway. From 1984 he has been involved with development of medical ultrasound imaging systems at Vingmed Sound A.S., where he currently holds the position as Director of Research. His research interests include signal processing with application to medical imaging and noninvasive diagnosis.